Silver halide fiber-based evanescent-wave liquid droplet sensing with room temperature mid-infrared quantum cascade lasers

J. Z. Chen, Z. Liu, and C. F. Gmachl

Princeton Institute for the Science and Technology of Materials (PRISM) and Department of Electrical Engineering, Princeton University, NJ 08544
jianchen@princeton.edu cgmachl@princeton.edu

D. L. Sivco

Bell Laboratories, Lucent Technologies, Murray Hill, NJ 07974

Abstract: Quantum cascade lasers and unclad silver halide fibers were used to assemble mid-infrared fiber-optics evanescent-wave sensors suitable to measure the chemical composition of liquid droplets. The laser wavelengths were chosen to be in the regions which offer the largest absorption contrast between constituents inside the mixture droplets. A pseudo-Beer-Lambert law fits well with the experimental data. Using a 300μm diameter fiber with a 25 mm immersion length, the signal to noise ratios correspond to 1 vol.% for α-tocophenol in squalane and 2 vol.% for acetone in aqueous solution for laser wavenumbers of 1208 cm^{-1} and 1363 cm^{-1}, respectively.

OCIS Codes: (060.2370) Fiber optics sensors; (280.3420) Laser sensors

References and Links

1. C. Gmachl, F. Capasso, D. L. Sivco, and A. Y. Cho, "Recent progress in quantum cascade lasers and applications," Rep. Prog. Phys. **64**, 1533 (2001).
2. C. Gmachl, F. Capasso, R. Köhler, A. Tredicucci, A. L. Hutchinson, D. L. Sivco, J. N. Baillargeon, and A. Y. Cho, "The sense-ability of semiconductor lasers – mid-infrared tunable quantum cascade lasers for gas-sensing applications," IEEE Circ. Dev. **16**, 10 (2000).
3. A. A. Kosterev and F. K. Tittel, "Chemical sensors based on quantum cascade lasers," IEEE J. Quantum Electron. **38**, 582 (2002).
4. C. Roller, A. A. Kosterev, F. K. Tittel, K. Uehara, C. Gmachl, and D. L. Sivco, "Carbonyl sulfide detection with a thermoelectric ally cooled midinfrared quantum cascade laser," Opt. Lett. **28**, 2052 (2003).
5. A. A. Kosterev, C. Roller, R. F. Curl, M. P. Fraser, and F. K. Tittel, "Monitoring of ethylene by a pulsed quantum cascade laser," Appl. Opt. **43**, 3329 (2004).
6. R. Jimenez, M. Taslakov, V. Simeonov, B. Calpini, F. Jeanneret, D. Hofstetter, M. Beck, J. Faist, and H. van den Bergh, "Ozone detection by differential absorption spectroscopy at ambient pressure with a 9.6 μm pulsed quantum-cascade laser," Appl. Phys. B **78**, 249 (2004).
7. L. Hvozdara, S. Gianordoli, G. Strasser, W. Schrenk, K. Unterrainer, E. Gornik, C. S. S. S. Murthy, M. Kraft, V. Pustogow, B. Mizaikoff, A. Inberg, and N. Croitoru, "Spectroscopy in the gas phase with GaAs/AlGaAs quantum-cascade lasers," Appl. Opt. **39**, 6926 (2000).
8. C. Charlton, F. de Melas, A. Inberg, N. Croitoru, and B. Mizaikoff, "Hollow-waveguide gas sensing with room-temperature quantumcascade lasers," IEE Proc. Optoelectron. **150**, 306 (2003).
9. B. Lendl, J. Frank, R. Schindler, A. Muller, M. Beck, and J. Faist, "Mid-infrared quantum cascade lasers for flow injection analysis," Anal. Chem. **72**, 1645 (2000).
10. M. Kolhed, M. Haberkorn, V. Pustogov, B. Mizaikoff, J. Frank, B. Karlberg, and B. Lendl, "Assessment of quantum cascade lasers a mid infrared light sources for measurement of aqueous samples," Vib. Spectrosc. **29**, 283 (2002).
11. A. Edelmann, C. Ruzicka, J. Frank, B. Lendl, W. Schrenk, E. Gornik, and G. Strasser, "Toward functional group-specific detection in high-performance liquid chromatography using mid-infrared quantum cascade lasers," J. Chromatogr. **934**, 123 (2001).
12. S. Schaden, M. Haberkorn, J. Frank, J. R. Baema, and B. Lendl, "Direct determination of carbon dioxide in aqueous solution using mid-infrared quantum cascade lasers," Appl. Spectrosc. **58**, 667 (2004).

#7198 - $15.00 US Received 19 April 2005; revised 23 June 2005; accepted 21 July 2005

13. J. Z. Chen, A. A. Darhuber, S. M. Troian, and S. Wagner, "Capacitive sensing of droplets for microfluidic devices based on thermocapillary actuation," Lab Chip **4**, 473 (2004).
14. A. A. Darhuber, J. P. Valentino, S. M. Troian, and S. Wagner, "Thermocapillary actuation of droplets on chemically patterned surfaces by programmable microheater arrays," J. Microelectromech. Sys. **12**, 873 (2003).
15. J. Z. Chen, S. M. Troian, A. A. Darhuber, and S. Wagner, "Effect of contact angle hysteresis on thermocapillary droplet actuation," J. Appl. Phys. **97**, 014906 (2005).
16. M. G. Pollack, R. B. Fair, and A. D. Shenderov, "Electrowetting-based actuation of liquid droplets for microfluidic applications," **77**, 1725 (2000).
17. P. G. de Gennes, "Wetting: statics and dynamics," **57**, 827 (1985).
18. S. S. Datwani, R. A. Vijayendran, E. Johnson, and S. A. Biondi, "Mixed alkanethiol self-assembled monolayers as substrates for microarraying applications," Langmuir **20**, 4970 (2004).
19. A. Messica, A. Greenstein, and A. Katzir, "Theory of fiber-optic, evanescent-wave spectroscopy and sensors," Appl. Opt. **35**, 2274 (1996).
20. J. S. Sanghera, F. H. Kung, P. C. Pureza, V. Q. Nguyen, R. E. Miklos, and I. D. Aggarwal, "Infrared evanescent-absorption spectroscopy with chalcogenide glass-fibers," Appl. Opt. **33**, 6315 (1994).

1. Introduction

Quantum Cascade Lasers (QCLs) have been the focus of much investigation over the past decade because of their many desirable properties. They can be operated in both continuous and pulsed mode with high optical power and at high temperature, which is a clear advantage over traditional semiconductor lasers in the same wavelength range; the wavelengths of QCLs can be designed anywhere in the mid-infrared range (roughly 3-25 μm), the spectroscopic fingerprint region of many interesting chemicals, which makes QCLs promising light sources for chemical sensing [1-3]. For sensing in the gas phase, direct absorption spectroscopic detection of trace gases using a multipass optical gas cell has been one of the main techniques for which QCLs have been tested, with many different groups reporting a plethora of methods for the sensing of specific gases [4-6]. Hollow waveguide gas sensing, in which the optical cell is a hollow fiber containing trace gas mixture, has been demostrated with detection limits of 250 ppm (ethene) and 5 ppm (ethyl chloride) for the waveguide lengths of 0.434 m and 4 m, respectively [7,8]. QCLs were also applied to direct absorption mesaurements in the liquid phase such as analyzing the phosphate [9], adenine/xanthosine [10], glucose/fructose [11], as well as CO_2 [12] level in aqueous solutions. In these measurements, intense optical power from the QCLs increases the useful optical path to hundreds of micrometers, while the optical signal will be completely absorbed within a few tens of micrometers using a conventional blackbody thermal source. The possible increase of the optical path length opens up an opportunity to apply compact QCLs as a light source in biochip or microfluidic devices, in which several hundreds of micrometers and even millimeter size liquid samples are used, as smaller samples would easily clog the channels for complex fluids.

To further increase the optical path length and examine the sensing capability of QCLs in the liquid phase, we investigate here the feasibility of fiber optics evanescent-wave liquid droplet-sensing using room temperature operated multimode QCLs coupled to a 300μm diameter unclad silver halide fiber. The fiber penetrated through liquid droplets as an evanescent sensing element. By matching the laser wavelength to the absorption maxima of various liquid samples, detection sensitive to the specific functional group or vibrational/bending modes of chemical bonds is achieved. The absorption coefficients of the liquids under test at specific wavelengths were also determined experimentally. The large signal to noise ratio of laser light (QCLs) allows much faster data sampling compared to measurements using a blackbody thermal source, which usually requires over one hundred scans to resolve good spectra using a commercial Fourier transform infrared spectrometer (FTIR).

We conducted our experiments in open space with the droplet sitting on a hydrophobic surface in order to mimic the case of *free surface (open channel)* droplet sensing on *free surface* microfluidic devices, such as thermally actuated microfluidic devices [13-15], electrowetting devices [16], or a proposed on-chip QCL-waveguide biochemical sensing

#7198 - $15.00 US Received 19 April 2005; revised 23 June 2005; accepted 21 July 2005

system. Here, there are two important issues which are different from closed flow cell sensing. First, presence of precursor films [17] on a wettable sensing element may affect the measurement. Second, the effects of substrates on the output signal need to be taken into account,

Free surface microfluidic devices usually require surface modifications. Silanization [13-15] and thiolation [18] are two commonly used methods. The former requires glass substrate while the latter needs Au (or metal) surface. In this paper, we also investigate substrate effects on the measured signal.

2. Experimental setup

Figure 1 shows a diagram of the experimental setup. Multimode Fabry-Perot type QCLs were placed on a thermoelectric cooling stage. For liquid sensing, multimode QCLs are sufficient since the absorption peaks of liquids are much broader than the laser emission spectrum. The wavelengths were thermally fine-tuned around room temperature to characteristic strong absorption features of the liquids under test. The laser was driven by an Agilent pulse current generator and directly coupled to a 12.7 cm long silver halide fiber. The output from the fiber was collimated by two Ge lenses onto a liquid nitrogen cooled HgCdTe (MCT) detector. The electrical detector signal was measured by a lock-in amplifier and recorded. The silver halide fiber rested on a surface onto which the liquid droplets were dispensed. The hydrophobic substrates were processed by depositing 1H,1H,2H,2H-perfluoro-octyltrichlorosilane (PFOTS, $C_8H_4Cl_3F_{13}S$) on pristine glass slides or hexadecanethiol (HDT, $C_{16}H_{34}S$) on Au-coated slides, respectively. The HDT/Au surface is highly reflective, whereas the PFOTS/glass surface is absorptive at the chosen wavelengths. These two surface coating reagents are commonly used for *free surface* microfluidic devices; the two different substrates were used to examine the effects of substrate reflectivity.

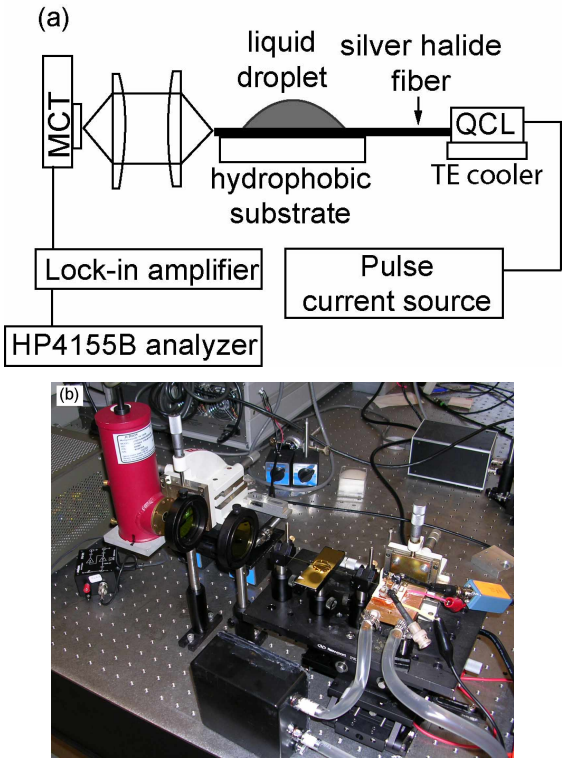

Fig. 1. (a) Drawing of experimental setup. (b) Photograph of experimental setup.

#7198 - $15.00 US Received 19 April 2005; revised 23 June 2005; accepted 21 July 2005

Figure 2(a) presents the emission spectra from the bare laser facet, and collected after the unclad or clad fiber under the same operation conditions. The 300μm diameter unclad fiber (MIR300) was purchased from CeramOptic. The 400μm/500μm core/clad fiber (PIR 400/500) was purchased from JT Ingram Inc. The fiber end was hand-cut with a razor blade and then hand polished with 1 μm Al_2O_3 powder. The spectra with and without fiber are essentially the same, with small variations similar to repeat measurements of the bare laser. Dispersion in the fiber is negligible across the small wavelength range and the energy exchange between mode does not occur since the fiber length is smaller than the coherence length $L_c \sim 1/\alpha_{AgX}$, where α_{AgX} is the absorption coefficient of the fiber (~0.6 dB/m). Coupling efficiencies to the fibers were measured through light-current-voltage (L-I-V) measurements, as shown in Fig. 2(b). The I-V measurement results are essentially identical with and without fibers. The L-I measurements were performed with clad and unclad fibers in comparison to the bare laser. The dotted lines represent the detected laser intensity with the fibers while the solid lines stand for the intensities of the bare lasers. After the laser was turned on, the coupling efficiency can be determined from the ratio of the optical power before and after the laser was coupled to the fiber. For an unclad fiber with a numerical aperture (NA) of 0.5, the coupling efficiency is determined as ~56%. The loss comes mainly from the Fresnel loss (~24%) at the fiber air interface and fiber losses. As for the clad fiber with a 0.25 NA, the coupling efficiency is measured to be ~41%. The additional loss is likely due to the large divergence angle of QCLs (~30^o - 60^o full width) such that the clad fiber with smaller NA cannot accommodate all light.

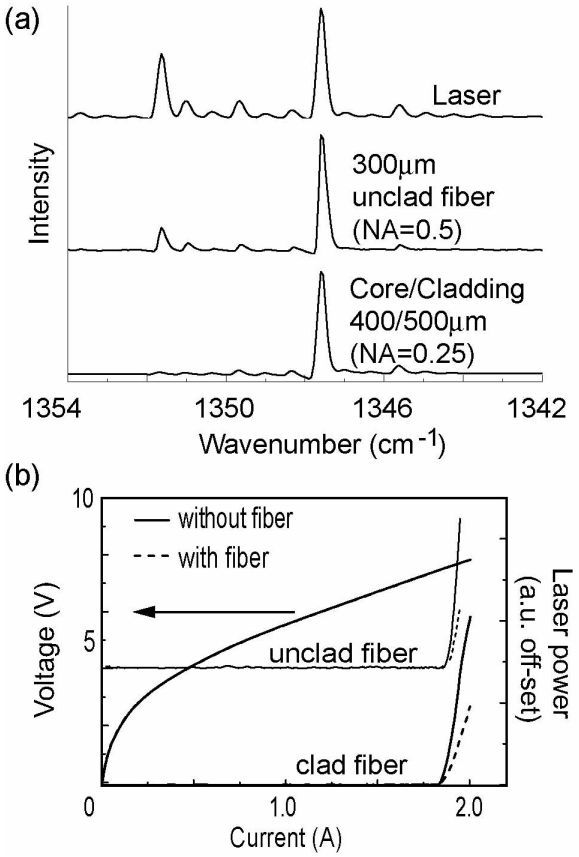

Fig. 2. (a) Comparison of FTIR spectra for the bare laser, and the laser coupled to an unclad fiber and clad fiber, respectively. (b) L-I-V measurements comparing the fiber coupled and un-coupled laser.

#7198 - $15.00 US Received 19 April 2005; revised 23 June 2005; accepted 21 July 2005

We chose common solvents and laboratory liquids, such as water, glycerol, acetone, ethanol, n-dodecane, squalane, and α-tocophenol acetate, to test this sensor setup. The α-tocophenol acetate/squalane mixture is selected because both are common ingredients of cosmetics, either as active ingredients or for chemical stabilization. The absorption coefficients of water, glycerol, α-tocophenol acetate, and squalane were measured by varying the immersion lengths. Concentration measurements of two sets of liquid solutions were tested, ethanol/water and acetone/water mixtures as representatives of aqueous solutions; n-dodecane/squalane and α-tocophenol acetate/squalane mixtures are oil-base solutions. n-dodecane/squalane is used as a control experiment to investigate the absorptive effect due to the difference of the refractive indexes of the various constituents.

3. Experimental results and discussion

3.1. Measurement of the absorption coefficients

Figure 3 shows experimental results for different liquids at various laser wavelengths, plotting the normalized transmitted intensity (I/I_o) over the fiber immersion length, i.e. the droplet size. Here I is the transmitted intensity in the presence of an absorber and I_o is the transmitted intensity through the bare fiber without surrounding liquid. Liquid immersion lengths were increased by increasing the volume of the droplet. The data are fitted with first order exponential decay functions with good result. This fitting implies that a pseudo-Beer-Lambert law [19,20] is applicable; this is a reasonable assumption for test liquids dissolved in non-absorptive media and fibers with high refractive index (~ 2.2) [19].

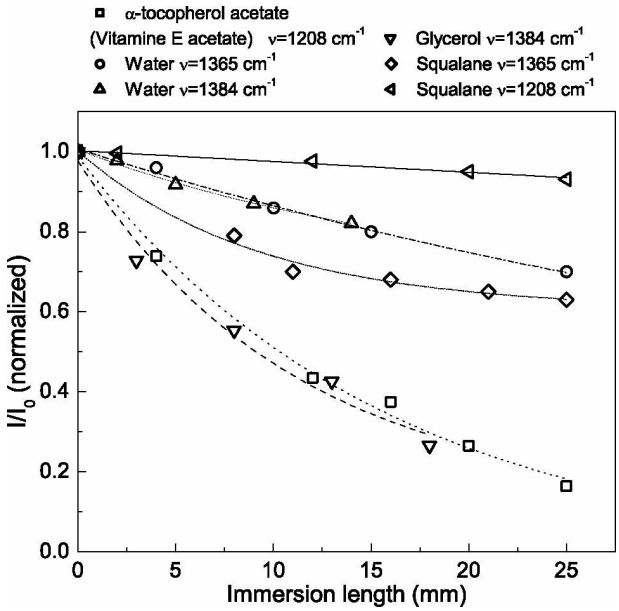

Fig. 3. Normalized transmitted intensity (I/I_0) as a function of immersion length for various liquids, where I_0 is the transmitted intensity in the absence of liquid. The symbols are the measured data. The lines are least square fits using an exponential decay fit function of $I/I_0 = \exp(-\alpha \cdot L)$, where α and L stand for the absorption coefficient and immersion length, respectively. Absorption coefficients (α's) of 0.64 cm^{-1} (α–tocophenol acetate at 1363 cm^{-1}), 0.15 cm^{-1} (squalane at 1363 cm^{-1}), 0.03 cm^{-1} (squalane at 1208 cm^{-1}), 0.68 cm^{-1} (glycerol at 1384 cm^{-1}), 0.55 cm^{-1} (water at 1363 cm^{-1}), and 0.53 cm^{-1} (water at 1384 cm^{-1}), are obtained from the exponential fits to the data..

3.2. Measurement of liquid concentrations

#7198 - $15.00 US Received 19 April 2005; revised 23 June 2005; accepted 21 July 2005

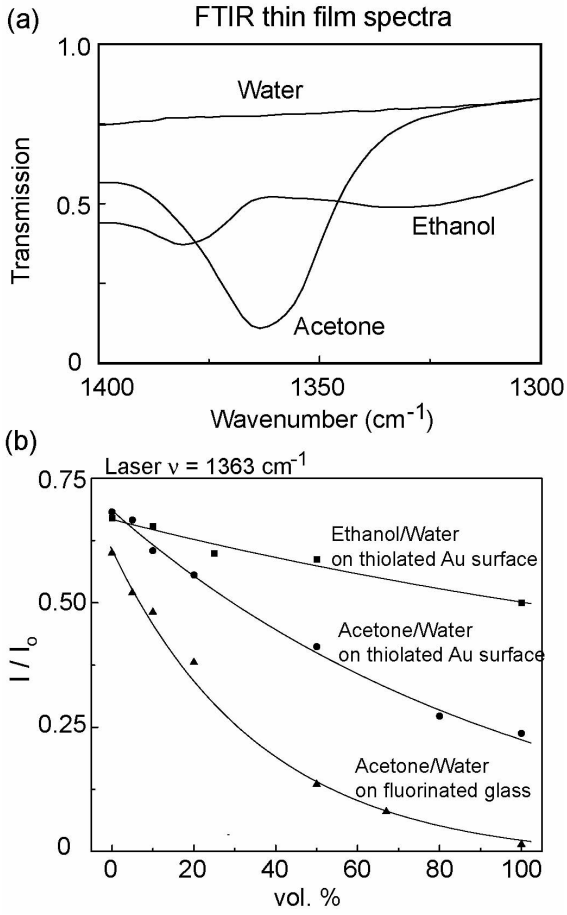

Fig. 4. (a) FTIR thin film transmission spectra of water, ethanol and acetone near the operating laser wavelength. (b) Normalized transmitted intensity (I/I_0) as a function of concentrations for ethanol/water and acetone/water mixtures at a laser wavelength of 1363 cm^{-1}, where I_0 is the transmitted intensity without liquid. The symbols are measured data; the lines are fitting functions. Fit functions: $y=0.253+0.415\cdot\exp(-x/196.1)$ for ethanol/water on HDT/Au/glass surface; $y=-0.0307+0.718\cdot\exp(-x/98.58)$ for acetone/water on HDT/Au/glass surface, and $y=0.613\cdot\exp(-x/35.41)$ for acetone/water on PFOT/glass surface, where y is normalized intensity (I/I_0) and x is the volumetric concentration in percentage.

Since the penetration depth into the liquid is rather small (~1-2μm in our case) because of the large fiber diameter, strong absorption occurs only when the absorption coefficient of the liquid is fairly high. Figures 4 and 5 present the measurements of normalized transmitted intensity versus concentration of several mixtures. Both thiolated Au slides (reflective surface) and fluorinated glass slides (absorptive surface) were used to test the effect of the substrate on the optical power received by the MCT detector. Figure 4 shows the results for an acetone/water mixture and an ethanol/water mixture. Acetone shows strong absorption around 1363 cm^{-1} resulting from an CH_3 bending vibration and around 1220 cm^{-1} resulting from the Ketone functional group, while ethanol also has bands near 1363 cm^{-1} arising from the CH, CH_2 and CH_3 bending vibrations as well as the OH bending vibration [20]. Nevertheless the absorption of ethanol at 1363 cm^{-1} is not as strong as that of acetone, as is indicated in thin film FTIR transmission spectra of Fig. 4(a). We chose 1363 cm^{-1} to match the maximum absorption of the analyte (acetone in this case) and compare the aqueous mixtures of the two different chemicals having different absorption coefficients. We performed concentration measurement with a liquid immersion length of 25 mm. As shown in Fig. 4(b), the

#7198 - $15.00 US Received 19 April 2005; revised 23 June 2005; accepted 21 July 2005

ethanol/water mixture absorbed less than the acetone/water mixture for the same concentration, as is also expected from the FTIR measurements in Fig. 4(a), in which acetone clearly shows stronger absorption than ethanol at this wavelength. As the concentration of ethanol or acetone increases, the transmitted intensity decreases because both ethanol and acetone have stronger absorption than water at 1363 cm^{-1}. The other reason is due to absorption maxima shifts as the concentration changes [20]. At the same acetone/water concentration, the transmitted intensity is smaller for droplets on PFOTS coated glass slides than on thiolated Au coated slides. This suggests that part of the light may be coupled into and absorbed by the glass slide via the thin liquid medium between the fiber and the glass slide. On the other hand, Au has very high reflectivity in the mid-infrared wavelength range, so that this coupling effect does not occur in the HDT/Au coated slide. We fit the normalized transmitted power as a function of concentration, as indicated in the figure captions. From the respective fit function, the concentration of the analyte can be determined.

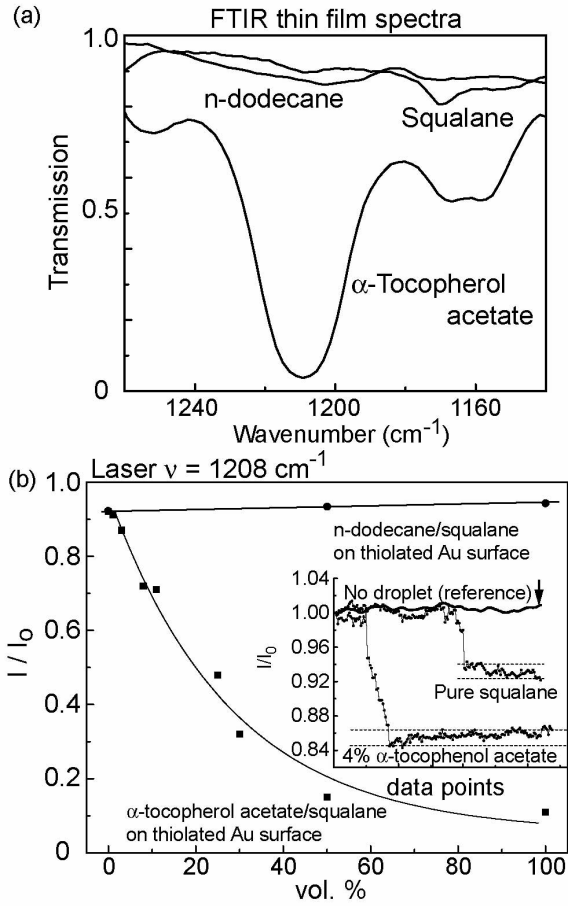

Fig. 5. (a) FTIR thin film spectra of squalane, n-dodecane and α–tocophenol acetate near the operating laser wavenumber. (b) Normalized transmitted intensity (I/I_0) as a function of the concentrations for n-dodecane/squalane and α–tocophenol acetate/squalane mixtures at a laser wavelength of 1208 cm^{-1}, where I_0 is the transmitted intensity without immersed liquid. Fit functions: y=0.97-0.048·exp(-x/173.80) for n-dodecane/squalane on HDT/Au/glass surface; y= -0.049+exp(-x/28.79) for α–tocophenol acetate/squalane on HDT/Au/glass surface. In these fitting functions, x stands for the vol.%, y represents the normalized transmitted intensity. Inset: Normalized transmitted intensity before and after dispensing droplets of pure squalane and squalane with 4% α-tocophenol acetate in it. In the presence of droplet, the normalized intensity decreases due to the absorbance of liquids.

#7198 - $15.00 US Received 19 April 2005; revised 23 June 2005; accepted 21 July 2005

Finally, we tested oil-based mixtures of n-dodecane ($C_{12}H_{26}$), squalane ($C_{30}H_{62}$) and α-tocophenol acetate ($C_{31}H_{52}O_3$, Vitamine E acetate). A control experiment was performed with an n-dodecane/squalane mixture. As can be seen in Fig. 5(b), the transmitted intensity in the latter case is a weakly dependent function of n-dodecane concentration, as no significant absorption occurs for either dodecane or squalane at the wavelength of 1208 cm^{-1} (8.28 μm). The effect of the refractive indices on the transmitted intensity is very small. With a fiber refractive index of 2.2, the differences of the liquid refractive indices (the refractive indices range from 1.3 to 1.5 for the liquids under test) only provide a small modification of the penetration depth into the liquid. This control experiment and FTIR spectra of individual chemicals ensure that the strong absorption of the α-tocophenol acetate/squalane mixture comes from the α-tocophenol acetate.

The sensitivity can be estimated from the signal to noise ratio of our experiment. The inset of Fig. 5(b) shows measured transmitted intensities before and after dispensing 25 mm diameter droplets of pure squalane and squalane with 4 vol.% α-tocophenol acetate in it. From these data, we extrapolate the signal to noise ratio to be about 1 vol.% concentration in the low concentration limit. At higher concentration, the intensity is less sensitive to the liquid composition. Therefore, the same noise level gives larger composition inaccuracy. The sensitivity and detection limit of acetone in water were estimated in the same fashion. In summary, with 25mm immersion length under low concentration condition, the signal to noise ratios correspond to 1 vol.% for α-tocophenol in squalane and 2 vol.% for acetone in aqueous solution at a laser wavenumber of 1208 cm^{-1} and 1363 cm^{-1}, respectively. In contrast, in attenuated total reflection measurements with chalcogenide glass-fibers and a conventional thermal IR source, a cylindrical fiber of 200 μm diameter and 180 mm immersion length were required to achieve 2% sensitivity for a similar solvent aqueous solution [20].

4. Conclusion

Room temperature operated Fabry-Perot type QCLs coupled to an unclad silver halide fiber were implemented as liquid droplet sensors. Using the lasers with designed wavelengths for specific chemicals, liquid compositions can be determined, if the absorption coefficients of components in the mixture have large contrast. Under low concentration conditions, using a 300 μm diameter silver halide fiber with a 25 mm droplet immersion length, the signal to noise ratio corresponds to 1 vol.% for α-tocophenol in squalane and 2 vol.% for acetone in aqueous solution for laser wavelengths of 1208 cm^{-1} and 1363 cm^{-1}, respectively.

This study was conducted as a precursor for a miniature integrated sensor system using QCLs and evanescent waveguide sensing. The sensitivity and detection limit can be further improved with a planar waveguide of thickness on the order of the laser wavelength, i.e. reaching the leaky waveguide limit.

Acknowledgments

This work was supported in part by the MRSEC grant at Princeton University, NSF-DMR 0213706, and by DARPA L-PAS.

#7198 - $15.00 US Received 19 April 2005; revised 23 June 2005; accepted 21 July 2005